Acta Pharmacologica Sinica (2010) 31: 1223–1240
 1671-4083/10 $32.00
www.nature.com/aps

Original Article

Regulation of Nrf2- and AP-1-mediated gene expression by epigallocatechin-3-gallate and sulforaphane in prostate of Nrf2-knockout or C57BL/6J mice and PC-3 AP-1 human prostate cancer cells

Sujit NAIR[1, 2, 3, 4], Avantika BARVE[1], Tin-Oo KHOR[1], Guo-xiang SHEN[1], Wen LIN[1], Jefferson Y CHAN[5], Li CAI[6], Ah-Ng KONG[1, *]

[1]Department of Pharmaceutics, Ernest Mario School of Pharmacy, Rutgers, The State University of New Jersey, Piscataway, NJ-08854, USA; [2]Division of Molecular Medicine, Amrita Centre for Nanosciences and Molecular Medicine, Amrita Institute of Medical Sciences and Research Centre, Amrita Vishwa Vidyapeetham University, Health Sciences Campus, Kochi-682041, Kerala, India; [3]Department of Pharmaceutics, Amrita School of Pharmacy, Amrita Vishwa Vidyapeetham University, Health Sciences Campus, Kochi-682041, Kerala, India; [4]Amrita School of Biotechnology, Amrita Vishwa Vidyapeetham University, Amritapuri Campus, Kollam-690525, Kerala, India; [5]Department of Pathology, University of California, Irvine, CA-92697, USA; [6]Department of Biomedical Engineering, Rutgers, The State University of New Jersey, Piscataway, NJ-08854, USA

Aim: To examine the regulatory crosstalk between the transcription factors Nrf2 and AP-1 in prostate cancer (PCa) by dietary cancer chemopreventive compounds (−)epigallocatechin-3-gallate (EGCG) from green tea and sulforaphane (SFN) from cruciferous vegetables.
Methods: We performed (i) *in vitro* studies including luciferase reporter gene assays, MTS cell viability assays, and quantitative real-time PCR (qRT-PCR) in PC-3 AP-1 human PCa cells, (ii) *in vivo* temporal (3 h and 12 h) microarray studies in the prostate of Nrf2-deficient mice that was validated by qRT-PCR, and (iii) *in silico* bioinformatic analyses to delineate conserved Transcription Factor Binding Sites (TFBS) in the promoter regions of Nrf2 and AP-1, as well as coregulated genes including ATF-2 and ELK-1.
Results: Our study shows that AP-1 activation was attenuated by the combinations of SFN (25 μmol/L) and EGCG (20 or 100 μmol/L) in PC-3 cells. Several key Nrf2-dependent genes were down-regulated (3-fold to 35-fold) after *in vivo* administration of the combination of EGCG (100 mg/kg) and SFN (45 mg/kg). Conserved TFBS signatures were identified in the promoter regions of Nrf2, AP-1, ATF2, and ELK-1 suggesting a potential regulatory mechanism of crosstalk between them.
Conclusion: Taken together, our present study of transcriptome profiling the gene expression changes induced by dietary phytochemicals SFN and EGCG in Nrf2-deficient mice and in PC-3 cells *in vitro* demonstrates that the effects of SFN+EGCG could be mediated via concerted modulation of Nrf2 and AP-1 pathways in the prostate.

Keywords: prostate cancer; sulforaphane; EGCG; Nrf2; AP-1; ATF-2; ELK-1; gene expression profiles

Acta Pharmacologica Sinica (2010) 31: 1223–1240; doi: 10.1038/aps.2010.147; published online 23 Aug 2010

Introduction

Prostate cancer (PCa), according to the Centers for Disease Control and Prevention (CDC)[1], is the second leading cause of cancer deaths among men in the United States, and the seventh leading cause of deaths overall for men. The incidence of PCa in the United States has increased by 1.1% per year from 1995–2003[1, 2]. In addition, the National Cancer Institute (NCI)'s Surveillance Epidemiology and End Results (SEER) Statistics Fact Sheets[3] show that, based on rates from 2002–2004, 16.72% of men born today will be diagnosed with cancer of the prostate at some time during their lifetime, *ie*, 1 in 6 men in the United States are at a lifetime risk of developing PCa. The prostate-specific antigen (PSA) nadir[4] while intermittently taking a testosterone-inactivating pharmaceutical agent has been determined to be the best predictor of prostate cancer-specific mortality. Nevertheless, despite the considerable attention given to PSA as a screening test for prostate cancer, it is needle biopsy, and not the PSA test result, that actually establishes the diagnosis of PCa[5].

Pivotal to the antioxidant response[6–9] typical in mammalian homeostasis and oxidative stress is the important transcription factor Nuclear Factor-E2-related factor 2 (Nrf2) that has

* To whom correspondence should be addressed.
E-mail kongt@rci.rutgers.edu
Received 2010-05-30 Accepted 2010-07-22

been extensively studied by many investigators including us, as noted elsewhere[10, 11]. Nrf2 is indispensable to cellular defense against many chemical insults of endogenous and exogenous origin, which play major roles in the etiopathogenesis of many cancers as well as inflammatory bowel disease[12] and Parkinson's disease[13]. Rushmore *et al*[14] were the first to identify a core antioxidant response element (core ARE or cARE) sequence 5′-RGTGACNNNGC-3′ responsible for transcriptional activation by xenobiotics, that was later expanded by Wasserman and Fahl[15] giving rise to an expanded ARE (eARE) sequence described by 5′-TMAnnRTGAYnnnGCRwwww-3′. We observed[16] that the induction of antioxidant response element (ARE)-regulated genes *in vitro* in human prostate cancer PC-3 cells upon treatment with phenethyl isothiocyanate (PEITC) is associated with the activation of extracellular signal-regulated kinase (ERK) and c-jun N-terminal kinase (JNK) resulting in the phosphorylation and nuclear translocation of Nrf2. Watai *et al*[17] showed that endogenous Keap1, which acts as a regulator of Nrf2 activity through an interaction with the Nrf2 Neh2 domain, remains mostly in the cytoplasm, and electrophiles promote nuclear accumulation of Nrf2 without altering the subcellular localization of Keap1. Thus, the Keap1-Nrf2-ARE axis potentially has an important role to play in various forms of cancer including that of the prostate.

AP-1 is a redox-sensitive transcription factor that senses and transduces changes in cellular redox status and modulates gene expression responses to oxidative and electrophilic stresses presumably via sulfhydryl modification of critical cysteine residues found on this protein and/or other upstream redox-sensitive molecular targets[10]. AP-1 is composed of heterodimeric protein complexes of members of the basic leucine zipper (bZIP) protein families, including the Jun (c-Jun, JunB, and JunD) and Fos (c-Fos, FosB, Fra-1, and Fra-2) families, Maf (c-Maf, MafB, MafA, Maf G/F/K, and Nrl), Jun dimerization partners (JDP1 and JDP2) and the closely related activation transcription factor (ATF; ATF2, LRF1/ATF3, and B-ATF) subfamilies[18–20] which recognize either 12-*O*-tetradecanoylphorbol-13-acetate (TPA) response elements (TRE, 5′-TGAG/CTCA-3′) or cAMP response elements (CRE, 5′-TGACGTCA-3′)[21]. We have shown that ERK and JNK signaling pathways are involved in the regulation of AP-1 and cell death elicited by three isothiocyanates (sulforaphane, SFN; PEITC; and allyl isothiocyanate, AITC) in human PCa PC-3 cells[19].

Evidence derived from epidemiological studies has revealed an inverse correlation between the intake of cruciferous vegetables and the risk of certain types of cancer[22]. Isothiocyanates are a chemical class of compounds that are not naturally present in cruciferous vegetables, such as broccoli and cauliflower, but are nevertheless generated from hydrolysis of secondary metabolites known as glucosinolates by the enzyme myrosinase during the process of vegetable crushing or mastication[23]. They may also be produced in the intestines where resident microflora can promote the hydrolysis of glucosinolates to isothiocyanates[24]. SFN, a dietary phytochemical obtained from broccoli, has been implicated in several physiological processes consistent with anticarcinogenic activity, including enhanced xenobiotic metabolism, cell cycle arrest, and apoptosis[25]. SFN has been shown[26] to retard the growth of human PC-3 xenografts and inhibit HDAC activity in human subjects. We have observed[27] that SFN induces hemoxygenase-1 (HO-1) by activating the antioxidant response element (ARE) through the induction of Nrf2 protein in HepG2 cells. It has also been reported[28] that SFN-induced cell death in PC-3 and DU145 human PCa cells is initiated by reactive oxygen species and that induction of autophagy[29] represents a defense mechanism against SFN-induced apoptosis in PC-3 and LNCaP human PCa cells. In addition, we have observed[30] that SFN suppresses the transcriptional activation of NF-κB as well as NF-κB-regulated gene expression in PC-3 cells via inhibition of IKKbeta phosphorylation as well as IkappaBalpha phosphorylation and degradation. Mass spectrometric methods have shown that SFN exists as the SFN-glutathione conjugates in enterocytes whereas the N-acetyl cysteine conjugate is the primary urinary metabolite[31].

The water-extractable fraction of green tea contains abundant polyphenolic compounds, in which (–)epigallocatechin-3-gallate (EGCG) is the major constituent (>50% of polyphenolic fraction)[32]. We have observed[33] that EGCG treatment causes damage to mitochondria, and that JNK mediates EGCG-induced apoptotic cell death in HT-29 human colon cancer cells. EGCG is also reported[34, 35] to inhibit DNA methyltransferase with demethylation of the CpG islands in the promoters, and to reactivate methylation-silenced genes such as p16INK4a, retinoic acid receptor beta, O6-methylguanine methyltransferase, human mutL homolog 1, and glutathione S-transferase-pi in human colon cancer HT-29 cells, esophageal cancer KYSE 150 cells, and PCa PC-3 cells. It was noted[36] that EGCG suppresses early stage, but not late stage, PCa in TRAMP (Transgenic Adenocarcinoma Mouse Prostate) animals without incurring undue toxicity. Besides, EGCG has been reported[37] to modulate the phosphatidylinositol-3-kinase/protein kinase B- and MAPK-pathways in DU145 and LNCaP human PCa cells, and to have combined inhibitory effects with selective cyclooxygenase-2 inhibitors[38] on the growth of human PCa cells both *in vitro* and *in vivo*. We have also shown[39] that a greater number of Nrf2-regulated genes are modulated in murine liver on oral administration of EGCG than in small intestine. Mass spectrometric methods have shown that EGCG produces methylated and conjugated metabolites in mice[40].

Nrf2 knockout mice are greatly predisposed to chemical-induced DNA damage and exhibit higher susceptibility towards cancer development in several models of chemical carcinogenesis[41]. In the present study, we investigated via transcriptome profiling the gene expression changes induced by a combination of dietary phytochemicals SFN and EGCG in Nrf2-deficient mice, the *in vitro* effects of this combination in PC-3 AP-1 cells, and delineated conserved Transcription Factor Binding Sites (TFBS) in the promoter regions of Nrf2 and AP-1, as well as coregulated genes including ATF-2 and

ELK-1, by *in silico* bioinformatic analyses. We demonstrate that the effects of the combination of SFN+EGCG in PCa may be mediated via concerted modulation of Nrf2 and AP-1 pathways.

Materials and methods

Cell culture and reagents

Human PCa PC-3 cells were stably transfected with an Activator Protein (AP-1) luciferase reporter construct, and are referred to as PC-3 AP-1 cells. The cells were cultured in Minimum Essential Medium (MEM) containing 10% Fetal Bovine Serum (FBS) and 1% Penicillin-Streptomycin. Twelve hours prior to experimental treatments, the cells were exposed to MEM containing 0.5% FBS. SFN was obtained from LKT Labs (St Paul, MN); whereas EGCG and superoxide dismutase (SOD) were obtained from Sigma-Aldrich (St Louis, MO). Both SFN and EGCG were dissolved in dimethylsulfoxide (DMSO, Sigma), whereas SOD was dissolved in 1×phosphate-buffered saline (PBS).

Reporter gene assays

PC-3 AP-1 cells were seeded in six-well culture plates and treated in triplicate with 0.1% dimethylsulfoxide (control), 20 μmol/L EGCG, 100 μmol/L EGCG, 25 μmol/L SFN, 20 μmol/L EGCG+25 μmol/L SFN, or 100 μmol/L EGCG+25 μmol/L SFN for 24 h. Thereafter, the supernatant medium was aspirated on ice, cells were washed thrice with ice-cold 1×PBS, treated with 1×Luciferase Reporter Lysis Buffer (Promega) and subjected to one cycle of snap freeze-thaw at -80 °C. Cell lysates were harvested with sterile RNAse-free and DNAse-free cell scrapers into microcentrifuge tubes that were immediately placed on ice. They were then centrifuged at 4 °C for ten minutes at 13000×*g* and returned to ice. Twenty microliters of supernatant solution was analyzed for relative luciferase activity using a Sirius Luminometer (Berthold Detection Systems). The relative luciferase activities were normalized by protein concentrations of individual samples determined as described below.

Protein assays

Protein concentrations of samples were determined by the bicinchonic acid-based BCA Protein Assay Kit (Pierce) according to the manufacturer's instructions using a 96-well plate. Standard curves were constructed using bovine serum albumin (BSA) as a standard. The sample readings were obtained on a μQuant microplate reader (Bio-tek Instruments Inc) at 560 nm.

Cell viability assays

The cell viability assays were performed in 24-well cell culture plates using MTS Assay Kit (Promega) according to the manufacturer's instructions. Cell viability was determined at both 24 and 48 h after treatment with dietary factors. The absorbance readings were obtained on an μQuant microplate reader (Bio-tek Instruments, Inc) at recommended wavelength of 490 nm.

RNA extraction and assessment of RNA integrity

PC-3 AP-1 cells were subjected to treatment with different dietary factors in triplicate for 6 or 10 h. RNA was harvested using the RNeasy Mini Kit (Qiagen) according to the manufacturer's instructions. RNA integrity was assessed using formaldehyde gels in 1×MOPS buffer and RNA concentration was determined by the 260/280 ratio on a DU 530 UV/Visible spectrophotometer (Beckman).

Quantitative real-time PCR assays

Several genes of interest including luciferase gene as well as genes known to be either under the control of the AP-1 promoter or involved in cell cycle regulation or cellular influx-efflux such as cyclin D1, cMyc, ATF-2, Elk-1, SRF, CREB5, MDR1, SLCO1B3, MRP1, MRP2, and MRP3 were selected for quantitative real-time PCR analyses. Beta-actin served as the "housekeeping" gene. The specific primers for these genes were designed using Primer Express 2.0 software (Applied Biosystems, Foster City, CA) and were obtained from Integrated DNA Technologies, Coralville, IA. The specificity of the primers was examined by a National Center for Biotechnology Information Blast search of the human genome. For the real-time PCR assays, briefly, after the RNA extraction and assessment of RNA integrity, first-strand cDNA was synthesized using 4 μg of total RNA following the protocol of SuperScript III First-Strand cDNA Synthesis System (Invitrogen) in a 40 μL reaction volume. The PCR reactions based on SYBR Green chemistry were carried out using 100 times diluted cDNA product, 60 nmol/L of each primer, and SYBR Green master mix (Applied Biosystems, Foster City, CA) in 10 μL reactions. The PCR parameters were set using SDS 2.1 software (Applied Biosystems, Foster City, CA) and involved the following stages : 50 °C for 2 min, 1 cycle; 95 °C for 10 min, 1 cycle; 95 °C for 15 s→55 °C for 30 s→72 °C for 30 s, 40 cycles; and 72 °C for 10 min, 1 cycle. Incorporation of the SYBR Green dye into the PCR products was monitored in real time with an ABI Prism 7900HT sequence detection system, resulting in the calculation of a threshold cycle (C_T) that defines the PCR cycle at which exponential growth of PCR products begins. The carboxy-X-rhodamine (ROX) passive reference dye was used to account for well and pipetting variability. A control cDNA dilution series was created for each gene to establish a standard curve. After conclusion of the reaction, amplicon specificity was verified by first-derivative melting curve analysis using the ABI software; and the integrity of the PCR reaction product and absence of primer dimers was ascertained. The gene expression was determined by normalization with control gene beta-actin.

Promoter analyses for transcription factor binding sites (TFBS)

The promoter analyses were performed using Genomatix MatInspector[42, 43]. Briefly, human promoter sequences of Nrf2, AP-1, ATF-2, and ELK-1, or corresponding murine promoter sequences, were retrieved from Gene2Promoter (Genomatix). Comparative promoter analyses were then performed by input of these sequences in FASTA format

into MatInspector using optimized default matrix similarity thresholds. The similar and/or functionally related TFBS were grouped into "matrix families" and graphical representations of common TFBS were generated. The 'V$' prefixes to the individual matrices are representative of the Vertebrate MatInspector matrix library. We also elucidated common regulatory sequences in promoter regions of human, or murine, Nrf2 and AP-1. The "core sequence" of a matrix is defined as the (usually four) highest conserved positions of the matrix that is provided in upper case letters in our Tables. The maximum core similarity of 1.0 is only reached when the highest conserved bases of a matrix match exactly in the sequence. Only matches that contain the "core sequence" of the matrix with a score higher than the core similarity are listed in the output.

Animals and dosing

The protocol for animal studies was approved by the Rutgers University Institutional Animal Care and Use Committee (IACUC). Nrf2 knockout mice Nrf2(–/–) (C57BL/SV129) have been described previously[44]. Nrf2(–/–) mice were backcrossed with C57BL/6J mice (The Jackson Laboratory, ME USA). DNA was extracted from the tail of each mouse and genotype of the mouse was confirmed by polymerase chain reaction (PCR) by using primers (3′-primer, 5′-GGA ATG GAA AAT AGC TCC TGC C-3′; 5′-primer, 5′-GCC TGA GAG CTG TAG GCC C-3′; and lacZ primer, 5′-GGG TTT TCC CAG TCA CGA C-3′). Nrf2(–/–) mice-derived PCR products showed only one band of ~200 bp, Nrf2 (+/+) mice-derived PCR products showed a band of ~300 bp while both bands appeared in Nrf2(+/–) mice PCR products. Male C57BL/6J/Nrf2(–/–) mice from third generation of backcross were used in this study. Age-matched male C57BL/6J mice were purchased from The Jackson Laboratory (Bar Harbor, ME). Mice in the age-group of 9–12 weeks were housed at Rutgers Animal Facility with free access to water and food under 12 h light/dark cycles. After one week of acclimatization, the mice were put on AIN-76A diet (Research Diets Inc, NJ) for another week. The mice were then administered both SFN (LKT Labs, St Paul, MN) and EGCG (Sigma-Aldrich, St Louis, MO) at doses of 45 and 100 mg/kg respectively (dissolved in 50% PEG 400 aqueous solution) by oral gavage. The control group animals were administered only vehicle (50% PEG 400 aqueous solution). Each treatment was administered to a group of four animals for both C57BL/6J and C57BL/6J/Nrf2(–/–) mice. Mice were sacrificed at either 3 h or 12 h after dietary factor treatment or vehicle administration (control group). The prostates of the animals were retrieved and stored in RNA Later (Ambion, Austin,TX) solution.

Microarray sample preparation and hybridization

Total RNA from prostate tissues was isolated by using TRIzol (Invitrogen, Carlsbad, CA) extraction coupled with the RNeasy kit from Qiagen (Valencia, CA). Briefly, tissues were homogenized in Trizol and then extracted with chloroform by vortexing. A small volume (1.2 mL) of aqueous phase after chloroform extraction and centrifugation was adjusted to 35% ethanol and loaded onto an RNeasy column. The column was washed, and RNA was eluted following the manufacturer's recommendations. RNA integrity was examined by electrophoresis, and concentrations were determined by UV spectrophotometry. Affymetrix (Affymetrix, Santa Clara, CA) Mouse Genome 430 2.0 array was used to probe the global gene expression profiles in mice following SFN+EGCG treatment. The Mouse Genome 430 2.0 Array is a high-density oligonucleotide array comprised of over 45 101 probe sets representing over 34 000 well-substantiated mouse genes. The library file for the above-mentioned oligonucleotide array is readily available at http://www.affymetrix.com/support/technical/libraryfilesmain.affx. After RNA isolation, the subsequent technical procedures including quality control and estimation of RNA concentration, cDNA synthesis and biotin-labeling of cRNA, hybridization and scanning of the arrays, were performed at CINJ Core Expression Array Facility of Robert Wood Johnson Medical School (New Brunswick, NJ). Each chip was hybridized with cRNA derived from a pooled total RNA sample from four mice per treatment group, per timepoint, and per genotype (a total of eight chips were used in this study). Briefly, double-stranded cDNA was synthesized from 5 μg of total RNA and labeled using the ENZO BioArray RNA transcript labeling kit (Enzo Life Sciences Inc, Farmingdale, NY) to generate biotinylated cRNA. Biotin-labeled cRNA was purified and fragmented randomly according to Affymetrix's protocol. Two hundred microliters of sample cocktail containing 15 μg of fragmented and biotin-labeled cRNA was loaded onto each chip. Chips were hybridized at 45 °C for 16 h and washed with fluidics protocol EukGE-WS2v5 according to Affymetrix's recommendation. At the completion of the fluidics protocol, the chips were placed into the Affymetrix GeneChip Scanner where the intensity of the fluorescence for each feature was measured.

Microarray data analyses

The CEL files (intensity DATA fields) were created from the scanned image and analyzed using dChip software[45, 46] for further data characterization. Briefly, a gene information file with current annotations and functional gene ontology was generated and the Affymetrix Chip Description File (CDF, information on the location and identity of different probe cells) was specified. The data were then normalized in dChip and the expression value for each gene was determined by calculating the average of differences in intensity (perfect match intensity minus mismatch intensity) between its probe pairs. The expression values were imported into GeneSpring 7.2 (Agilent Technologies Inc, Palo Alto, CA) followed by data filtration based on flags present in at least one of the samples, and a corresponding gene list based on those flags was generated. Lists of genes that were either induced or suppressed more than three fold between treated versus vehicle group of same genotype were created by filtration-on-fold function within the presented flag list. By use of Venn Diagram function, lists of genes that were regulated more than three fold only in prostate of C57BL/6J mice but not in prostate of C57BL/6J/

Nrf2(–/–) mice at both 3 and 12 h were generated, and were designated as Nrf2-dependent genes. The Affymetrix Probe Set IDs for the Nrf2-dependent genes were matched against the "all genes" expression values list for these set of samples, and expression values for these Affymetrix Probe Set IDs were retrieved. This "external data" was then imported into dChip whereupon Clustering and Enrichment Analysis was performed to obtain hierarchical tree clustering diagrams for the Nrf2-dependent genes. This clustering provided functional classification of Affymetrix Probe Set IDs and gene descriptions that were then matched with the GeneSpring-generated Nrf2-dependent Affymetrix Probe Set IDs with fold-change values. Quantitative real-time PCR assays as described earlier were performed on several genes to validate the microarray results.

Statistical analyses

Data are expressed as mean ± standard deviation, and comparisons among treatment groups were made using one-way analysis of variance (ANOVA) followed by a *post hoc* test for multiple comparisons — the Tukey's Studentized Range Honestly Significant Difference (HSD) test. In all these multiple comparisons, $P<0.05$ was considered statistically significant. In order to validate the microarray results, the correlation between corresponding microarray data and real-time PCR data was evaluated by r^2, the statistical "coefficient of determination" ($r^2=0.96$). Statistical analyses were performed using SAS 9.1 software (SAS Institute Inc, NC) licensed to Rutgers University.

Results

Diminished transactivation of AP-1 luciferase reporter by combinations of SFN and EGCG

As shown in Figure 1A, treatment of PC-3 AP-1 cells for 24 h with either 25 μmol/L SFN, 100 μmol/L EGCG or 20 μmol/L EGCG individually resulted in variable induction of AP-1 luciferase activity as compared to control cells that were treated with DMSO. Surprisingly, a low-dose combination of 25 μmol/L SFN+20 μmol/L EGCG elicited a diminished induction of AP-1 luciferase activity (less than 5-fold). In addition, a high-dose combination of 25 μmol/L SFN+100 μmol/L EGCG further diminished the induction of the AP-1 luciferase reporter. We also investigated the effects of pre-treatment on the induction of AP-1 luciferase activity. In these experiments (data not shown), we first pre-treated the PC-3 AP-1 cells for 6 h with EGCG (20 μmol/L or 100 μmol/L), then washed off the EGCG thrice with phosphate-buffered saline (PBS) and treated the cells with 25 μmol/L SFN for an additional 18 h before assaying for luciferase activity. Alternatively, we also pre-treated the cells with 25 μmol/L SFN for 6 h before washing with PBS as above and treating with EGCG (20 μmol/L or 100 μmol/L) for an additional 18 h. It was observed that there was no significant difference in induction of AP-1 luciferase activity in these pre-treatment experiments (data not shown) as compared to when the two agents were co-treated as shown in Figure 1A. This enabled us to rule out any physicochemical interaction between the two agents in cell culture, when co-treated, that may have otherwise produced any experimental artifacts in the luciferase assay. Hence, since the effects of the combinations when co-treated were not physicochemical, but potentially modulated at a mechanistic level, we continued co-treating both agents together for a duration of 24 h for ease of experimentation without confounding variables.

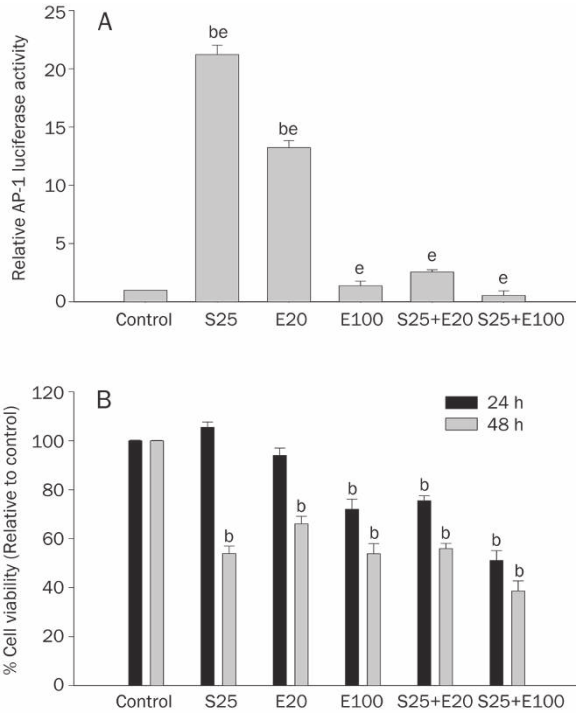

Figure 1. (A) Diminished transactivation of AP-1 luciferase reporter by combinations of SFN and EGCG. PC-3 AP-1 cells were seeded in six-well plates and treated with individual dietary factors, or with combinations of SFN and EGCG, as indicated (S25, sulforaphane 25 μmol/L; E20, EGCG 20 μmol/L; E100, EGCG 100 μmol/L). The AP-1 luciferase activity was measured relative to vehicle control (DMSO) after 24 h of incubation and normalized against protein concentration. Values represent mean± standard deviation for three replicates, and are representative of seven independent experiments. $^{b}P<0.05$ *vs* vehicle control; $^{e}P<0.05$, significantly different from each other. (B) Viability of the PC-3 AP-1 cells with the combinations of SFN and EGCG. PC-3 AP-1 cells were treated with individual dietary factors or with combinations of SFN and EGCG for 24 h or 48 h, as indicated, and treated with MTS assay reagent to ascertain cell viability (S25, sulforaphane 25 μmol/L; E20, EGCG 20 μmol/L; E100, EGCG 100 μmol/L). Values represent mean±standard deviation for six replicates, and are representative of three independent experiments. $^{b}P<0.05$ *vs* control.

Viability of the PC-3 AP-1 cells with the combinations of SFN and EGCG

In order to ascertain the effects of the combinations of SFN and EGCG on the cell viability of the PC-3 AP-1 cells, we used the MTS assay with treatment durations of 24 h and 48 h. As shown in Figure 1B, the cell viability at 24 h for the low-dose combination treatment of 25 μmol/L SFN+20 μmol/L EGCG was about 75% to 80%, whereas it was about 60% for the high-

dose combination of 25 μmol/L SFN+100 μmol/L EGCG. The low-dose combination of 25 μmol/L SFN+20 μmol/L EGCG may be more appropriate to pursue in longer duration *in vitro* studies or potential *in vivo* studies without seemingly toxic effects a priori, and at the same time not compromising on the efficacy elicited by the combination of these two chemopreventive agents.

Temporal gene expression profiles elicited by combinations of SFN and EGCG

We performed quantitative real-time PCR (qRT-PCR) experiments with primers for the luciferase gene to corroborate the synergism elicited with the combinations of SFN and EGCG in the luciferase protein assay with mRNA levels in qRT-PCR. The temporal expression (at 6 h and 10 h) of luciferase gene in qRT-PCR assays (Figure 2A) was lower for the combinations of SFN and EGCG as compared to individual dietary factor treatments in consonance with our data in the luciferase protein assays (Figure 1A). The treatment means for all the treatment groups at a specific time point (6 h or 10 h) were significantly different from each other ($P<0.05$ by ANOVA and *post hoc* Tukey's test for multiple comparisons to detect significantly different means). We also determined by qRT-PCR the relative expression levels of transcripts of many genes that were known to be either under the control of the AP-1 promoter or involved in cell cycle regulation or cellular influx-efflux such as cyclin D1, cMyc, ATF-2, ELK-1, SRF, CREB5, SLCO1B3, MRP1, MRP2, and MRP3 (Figure 2).

The low- and high-dose combinations of SFN and EGCG in this study elicited the downregulation of positive cell cycle regulator cyclin D1 expression as compared with individual dietary factors especially at 10 h (Figure 2B). There was, however, no appreciable change in expression of cell proliferation-related cMyc Binding Protein (Figure 2C). In addition, transcription factors/coactivators that are known to be under the control of the AP-1 promoter such as activating transcription factor (ATF-2), Ets-like transcription factor (ELK-1), serum response factor (SRF) and cyclic AMP response element binding protein 5 (CREB5) were also studied. Interestingly, both ATF-2 and ELK-1 were significantly downregulated by the combinations of SFN and EGCG as compared to individual dietary factors (Figure 2D and 2E). Besides, the low-dose combination of SFN and EGCG at 6 h (and the high-dose combination at 10 h) inhibited the expression of SRF as compared to individual dietary factors (Figure 2F). Similarly, the combinations inhibited the expression of CREB5 as compared to individual agents (Figure 2G). Since exogenous stress can potentially stimulate the influx-efflux machinery of cells, we also investigated some key transporter genes. In this study, we observed that the combinations of SFN and EGCG inhibited the SFN-induced expression of the SLCO1B3 gene, which encodes for the organic anion transporter protein OATP1B3, whereas the combinations did not have any clear effect on the expression of MDR1 gene (Figure 2H and 2I). Interestingly, the combinations of SFN and EGCG greatly induced the expression of the efflux transporter MRP2 as compared to individual dietary factors SFN or EGCG (Figure 2K). In addition, the expression of influx transporters MRP1 and MRP3 was not significantly different for the combination-treated cells as compared to the individual agent-treated cells (Figure 2J and 2L).

Comparative promoter analyses of Nrf2 and AP-1, as well as ATF-2 and ELK-1, for conserved Transcription Factor Binding Sites (TFBS)

We performed comparative analyses of Nrf2 and AP-1 human promoter sequences as described in Materials and Methods. We also studied Nrf2 and AP-1 murine promoter sequences similarly. We have alphabetically listed the conserved vertebrate (V$) matrix families between these two transcription factors in Table 1. The major human families included Activator protein 4 and related proteins, cell cycle regulators, E-box binding factors, human and murine ETS1 factors, fork head domain factors, hypoxia inducible factor, myc-associated zinc fingers, nuclear respiratory factor 1, serum response element binding factor, and signal transducer and activator of transcription amongst others. Interestingly, NF-κB was conserved in human sequences of Nrf2 and AP-1. We also performed comparative promoter analyses on ATF-2 and ELK-1 which are AP-1-regulated genes. We have alphabetically listed the conserved vertebrate (V$) matrix families between ATF-2 and ELK-1 in Table 2 and have provided a pictorial representation in Figures 3A and 3B. Some key conserved matrix families included AP-1, cyclic AMP-responsive element binding proteins, estrogen response elements, human and murine ETS1 factors, fork head domain factors, farnesoid-X-activated receptor response elements, human acute myelogenous leukemia factors, Ikaros zinc finger family, myc-associated zinc fingers, nuclear factor of activated T-cells, NF-κB, peroxisome proliferators-activated receptor, ras-responsive element binding protein, serum response element binding factor, signal transducer and activator of transcription, and X-box binding factors amongst others. Interestingly, as is evident from Tables 1 and 2, several key matrix families were conserved not just between Nrf2 and AP-1, or between the AP-1-regulated genes ATF-2 and ELK-1, in either human or murine species, but there was also some degree of overlap between TFBS identified in Tables 1 and 2. Furthermore, as shown in the Supplementary Table, we identified matrices (individual matrix family members) with conserved regulatory sequences in promoter regions of Nrf2 and AP-1 in either human or murine species. Multiple matches that were elicited with the same core sequence have also been grouped together and listed in the Supplementary Table.

Temporal microarray analyses of genes modulated by SFN+EGCG combination in the prostate of Nrf2-deficient mice

We clustered the genes that were downregulated at both 3 h and 12 h by the SFN+EGCG combination in the prostate of Nrf2-deficient mice according to their biological functions and listed them in Table 3. Interestingly, downregulation of genes appeared more important in the prostate of these

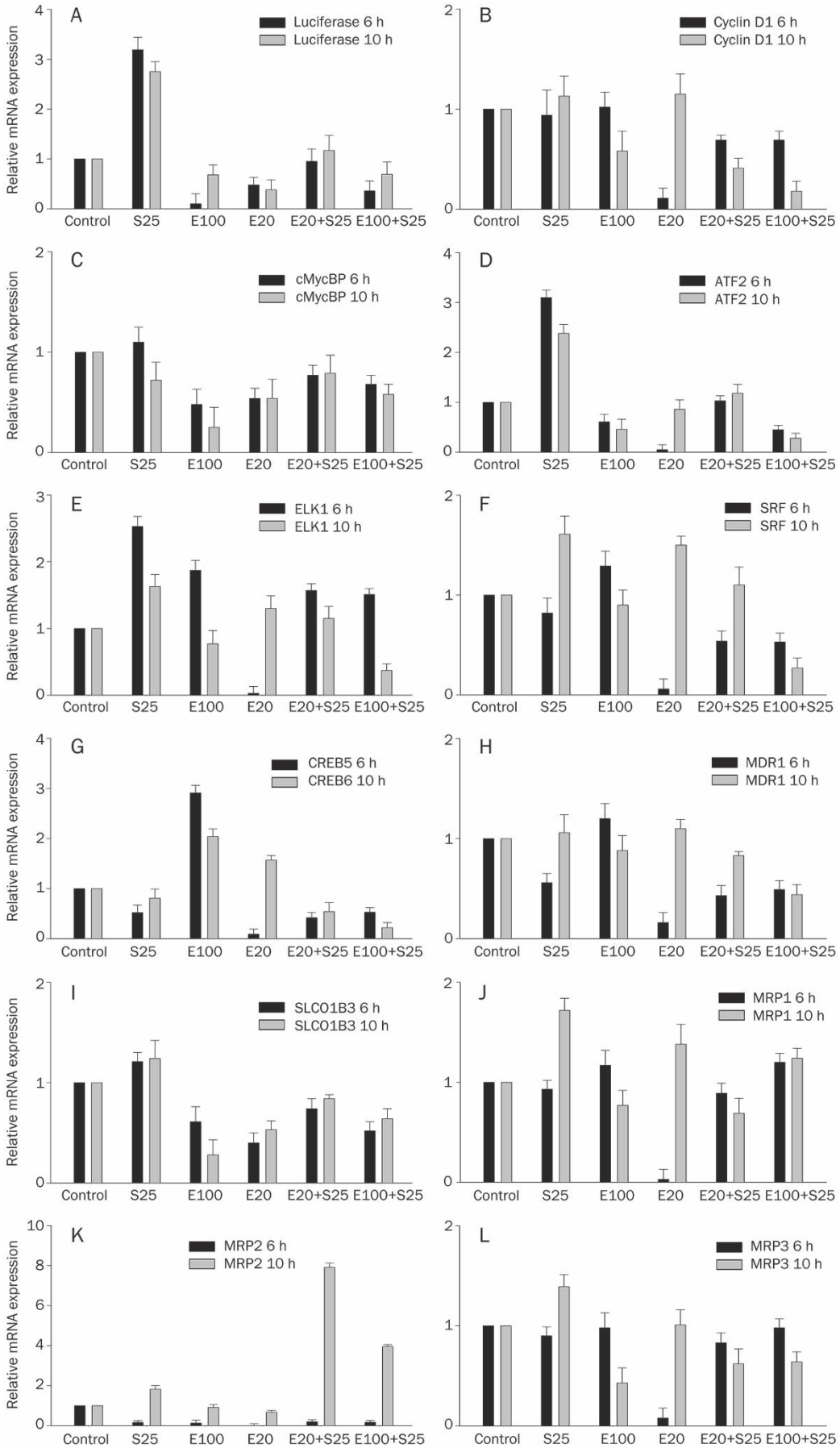

Figure 2. Temporal gene expression profiles elicited by combinations of SFN and EGCG. PC-3 AP-1 cells were treated for 6 h or 10 h with individual dietary factors, or combinations of SFN and EGCG, as indicated (S25, sulforaphane 25 μmol/L; E20, EGCG 20 μmol/L; E100, EGCG 100 μmol/L). RNA was extracted, transcribed into cDNA after ascertaining RNA integrity, and quantitative real-time PCR assays were performed for twelve genes at both time-points, as indicated, using beta-actin as the housekeeping gene. Values represent mean±standard deviation for three replicates of each gene, and are representative of two independent experiments.

Table 1. Human and murine matrix families conserved between Nrf2 and AP-1.

Matrix family human Nrf2 *vs* AP-1	Matrix family murine Nrf2 *vs* AP-1	Family information
V$AP4R	V$AP4R	Activator protein 4 and related proteins
V$CDEF	-	Cell cycle regulators: Cell cycle dependent element
V$CHRF	-	Cell cycle regulators: Cell cycle homology element
-	V$CP2F	CP2-erythrocyte factor related to drosophila Elf1
V$E2FF	-	E2F-myc activator/cell cycle regulator
-	V$E4FF	Ubiquitous GLI - Krueppel like zinc finger involved in cell cycle regulation
V$EBOX	–	E-box binding factors
V$EGRF	V$EGRF	EGR/nerve growth factor induced protein C & related factors
–	V$EKLF	Basic and erythroid krueppel like factors
–	V$ETSF	Human and murine ETS1 factors
V$EVI1	–	EVI1-myleoid transforming protein
–	V$FKHD	Fork head domain factors
V$GATA	–	GATA binding factors
–	V$GLIF	GLI zinc finger family
–	V$GREF	Glucocorticoid responsive and related elements
V$HAND	–	bHLH transcription factor dimer of HAND2 and E12
–	V$HESF	Vertebrate homologues of enhancer of split complex
–	V$HIFF	Hypoxia inducible factor, bHLH/PAS protein family
–	V$HNF6	Onecut homeodomain factor HNF6
–	V$INSM	Insulinoma associated factors
V$MAZF	V$MAZF	Myc associated zinc fingers
–	V$MOKF	Mouse Krueppel like factor
V$MYBL	–	Cellular and viral myb-like transcriptional regulators
V$MYOD	V$MYOD	Myoblast determining factors
V$NEUR	–	NeuroD, Beta2, HLH domain
V$NFKB	–	NF-κB/c-rel
V$Nrf1	V$Nrf1	Nuclear respiratory factor 1
V$PAX5	–	PAX-5 B-cell-specific activator protein
V$PAX9	–	PAX-9 binding sites
V$PBXC	–	PBX1 - MEIS1 complexes
–	V$PLAG	Pleomorphic adenoma gene
–	V$SF1F	Vertebrate steroidogenic factor
V$SP1F	V$SP1F	GC-Box factors SP1/GC
–	V$SRFF	Serum response element binding factor
V$STAF	–	Selenocysteine tRNA activating factor
V$STAT	–	Signal transducer and activator of transcription
–	V$XBBF	X-box binding factors
V$ZBPF	V$ZBPF	Zinc binding protein factors
–	V$ZF35	Zinc finger protein ZNF35

mice, since the upregulation of genes was negligible (data not shown). Indeed, a strong degree of downregulation ranging from 3 to around 35 fold was observed *in vivo*. This was also in consonance with our *in vitro* results in Figure 1A where the combination of SFN+EGCG elicited diminished activation of the luciferase reporter. Furthermore, several genes that were downregulated in our *in vivo* study were also common to our regulatory comparative promoter analyses between Nrf2 and AP-1, and ATF-2 and ELK-1, as described earlier. These included Ikaros family zinc fingers, forkhead box members, and ATF-2 amongst others. Interestingly, several coactivators and corepressors of Nrf2, as well as Nrf3, and the adenomatosis polyposis coli (Apc) gene, were also shown to be modulated via Nrf2 in response to the combination of SFN+EGCG.

Discussion

Expression profiling and proteomics have been credited[47] with the potential to transform the management of PCa by identifying new markers for screening, diagnosis, prognosis, monitoring and targets for therapy. Several studies have addressed the putative role(s) of either Nrf2 or AP-1 in PCa; however, the potential for putative crosstalk between these two important transcription factors in the pathogenesis of PCa has not been explored so far. In order to better appreciate the regulatory potential for concerted modulation of Nrf2 and AP-1 in PCa on treatment with dietary factors SFN and EGCG

Table 2. Human and murine matrix families conserved between ATF-2 and ELK1.

Matrix family human ATF2 *vs* ELK1	Matrix family murine Atf2 *vs* Elk1	Family information
V$AP1F	–	AP1, activator protein 1
–	V$BARB	Barbiturate-inducible element box from pro+eukaryotic genes
–	V$BNCF	Basonuclein rDNA transcription factor (PolI)
–	V$BRNF	Brn POU domain factors
V$CAAT	–	CCAAT binding factors
–	V$CLOX	CLOX and CLOX homology (CDP) factors
V$COMP	–	Factors which cooperate with myogenic proteins
–	V$CP2F	CP2-erythrocyte factor related to drosophila Elf1
V$CREB	–	Camp-responsive element binding proteins
–	V$E2FF	E2F-myc activator/cell cycle regulator
V$EBOX	–	E-box binding factors
V$EGRF	–	EGR/nerve growth factor induced protein C & related factors
V$EKLF	–	Basic and erythroid krueppel like factors
V$EREF	–	Estrogen response elements
V$ETSF	V$ETSF	Human and murine ETS1 factors
–	V$EVI1	EVI1-myleoid transforming protein
V$FKHD	V$FKHD	Fork head domain factors
–	V$FXRE	Farnesoid X-activated receptor response elements
–	V$GATA	GATA binding factors
–	V$GCMF	Chorion-specific transcription factors with a GCM DNA binding domain
V$GFI1	–	Growth factor independence transcriptional repressor
V$GKLF	V$GKLF	Gut-enriched Krueppel like binding factor
V$GLIF	–	GLI zinc finger family
–	V$HAML	Human acute myelogenous leukemia factors
–	V$HOXC	HOX-PBX complexes
–	V$HOXF	Factors with moderate activity to homeo domain consensus sequence
–	V$IKRS	Ikaros zinc finger family
V$IRFF	V$IRFF	Interferon regulatory factors
V$LEFF	V$LEFF	LEF1/TCF, involved in the Wnt signal transduction pathway
V$MAZF	–	Myc associated zinc fingers
–	V$MEF2	MEF2, myocyte-specific enhancer binding factor
V$MYBL	–	Cellular and viral myb-like transcriptional regulators
–	V$MYT1	MYT1 C2HC zinc finger protein
V$MZF1	–	Myeloid zinc finger 1 factors
V$NBRE	–	NGFI-B response elements, nur subfamily of nuclear receptors
–	V$NFAT	Nuclear factor of activated T-cells
V$NFKB	–	NF-κB/c-rel
V$NKXH	V$NKXH	NKX homeodomain factors
V$NR2F	V$NR2F	Nuclear receptor subfamily 2 factors
–	V$OCT1	Octamer binding protein
V$PARF	V$PARF	PAR/bZIP family
V$PAX5	–	PAX-5 B-cell-specific activator protein
V$PAX6	–	PAX-4/PAX-6 paired domain binding sites
V$PBXC	–	PBX1 - MEIS1 complexes
V$PERO	–	Peroxisome proliferator-activated receptor
–	V$PLZF	C2H2 zinc finger protein PLZF
V$RREB	–	Ras-responsive element binding protein
V$RXRF	–	RXR heterodimer binding sites
V$SNAP	–	snRNA-activating protein complex
V$SP1F	–	GC-Box factors SP1/GC
–	V$SRFF	Serum response element binding factor
V$STAF	–	Selenocysteine tRNA activating factor
–	V$STAT	Signal transducer and activator of transcription
V$TALE	–	TALE homeodomain class recognizing TG motifs
–	V$TBPF	Tata-binding protein factor
–	V$TEAF	TEA/ATTS DNA binding domain factors
–	V$XBBF	X-box binding factors
V$ZBPF	–	Zinc binding protein factors

Table 3. Temporal microarray analyses of genes modulated by SFN+EGCG combination in the prostate of Nrf2-deficient mice.

GenBank accession No	Gene symbol	Gene title	Prostate 3 h[a]	Prostate 12 h[b]
Apoptosis and cell cycle				
NM_019816	Aatf	Apoptosis antagonizing transcription factor	–	3.09
NM_007466	Api5	Apoptosis inhibitor 5	–	7.26
NM_007609	Casp4	Caspase 4, apoptosis-related cysteine peptidase	–	4.24
NM_011997	Casp8ap2	Caspase 8 associated protein 2	–	4.67
NM_026201	Ccar1	Cell division cycle and apoptosis regulator 1	–	3.31
NM_027545	Cwf19l2	CWF19-like 2, cell cycle control (S pombe)	–	3.48
NM_001037134	Ccne2	Cyclin E2	–	4.04
NM_009831	Ccng1	Cyclin G1	–	3.82
NM_028399	Ccnt2	Cyclin T2	–	3.16
NM_145991	Cdc73	Cell division cycle 73, Paf1/RNA polymerase II complex component, homolog (S cerevisiae)	–	6.13
Calcium ion binding				
NM_009722	Atp2a2	ATPase, Ca^{2+} transporting, cardiac muscle, slow twitch 2	–	3.14
NM_009784	Cacna2d1	Calcium channel, voltage-dependent, alpha2/delta subunit 1	–	4.81
NM_007977	F8	Coagulation factor VIII	–	4.18
NM_007868	Dmd	Dystrophin, muscular dystrophy	–	3.21
NM_007943	Eps15	Epidermal growth factor receptor pathway substrate 15	–	5.26
NM_001039644	Edem3	ER degradation enhancer, mannosidase alpha-like 3	–	4.54
NM_010427	Hgf	Hepatocyte growth factor	–	4.49
XM_001472723	Macf1	Microtubule-actin crosslinking factor 1	–	3.96
NM_011110	Pla2g5	Phospholipase A2, group V	–	3.89
NM_013829	Plcb4	Phospholipase C, beta 4	–	3.94
NM_009048	Reps1	RalBP1 associated Eps domain containing protein	–	6.19
NM_021450	Trpm7	Transient receptor potential cation channel, subfamily M, member 7	–	4.46
Digestion				
NM_025583	Ctrb1	Chymotrypsinogen B1	–	4.43
NM_025469	Clps	Colipase, pancreatic	–	3.85
NM_009430	Prss2	Protease, serine, 2	–	28.91
Extracellular space				
NM_009692	Apoa1	Apolipoprotein A–I	–	9.72
NM_018782	Calcrl	Calcitonin receptor-like	–	5.1
NM_001042611	Cp	Ceruloplasmin	–	3.77
NM_019919	Ltbp1	Latent transforming growth factor beta binding protein 1	–	3.46
NM_001039094	Negr1	Neuronal growth regulator 1	–	3.15
NM_011964	Psg19	Pregnancy specific glycoprotein 19	–	8.93
NM_009936	Col9a3	Procollagen, type IX, alpha 3	-	3.48
NM_001081385	Pcdh11x	Protocadherin 11 X-linked	–	8.52
NM_053141	Pcdhb16	Protocadherin beta 16	–	3.17
NM_021289	Smr2	Submaxillary gland androgen regulated protein 2	–	29.55
Integral to plasma membrane				
NM_008309	Htr1d	5-hydroxytryptamine (serotonin) receptor 1D	10.02	–
NM_008427	Kcnj4	Potassium inwardly-rectifying channel, subfamily J, member 4	3.49	–
NM_008422	Kcnc3	Potassium voltage gated channel, Shaw-related subfamily, member 3	11.48	–
NM_008434	Kcnq1	Potassium voltage-gated channel, subfamily Q, member 1	3.34	–
NM_001098170	Pcdh10	Protocadherin 10	4.1	–
BC098457	Pcdhgc3	Protocadherin gamma subfamily C, 3	3.5	–
AK041751	Tcrb-J	T-cell receptor beta, joining region	11.66	–
NM_029975	Ulbp1	UL16 binding protein 1	3.57	–
Intracellular				
NM_007478	Arf3	ADP-ribosylation factor 3	–	4.82

(Continued)

GenBank accession No	Gene symbol	Gene title	Prostate 3 h[a]	Prostate 12 h[b]
NM_134037	Acly	ATP citrate lyase	–	4.49
NM_015802	Dlc1	Deleted in liver cancer 1	3.23	–
NM_178118	Dixdc1	DIX domain containing 1	8.24	3.65
NM_007961	Etv6	Ets variant gene 6 (TEL oncogene)	4.57	–
NM_080433	Fezf2	Fez family zinc finger 2	–	3.44
NM_053202	Foxp1	Forkhead box P1	–	3.09
NM_175143	Qrich1	Glutamine-rich 1	4.75	–
NM_178888	Garnl3	GTPase activating RANGAP domain-like 3	3.02	–
NM_001025597	Ikzf1	IKAROS family zinc finger 1	13.8	–
NM_011771	Ikzf3	IKAROS family zinc finger 3	–	5.44
NM_016889	Insm1	Insulinoma-associated 1	4.07	–
NM_029416	Klf17	Kruppel-like factor 17	3.25	–
NM_053158	Mrpl1	Mitochondrial ribosomal protein L1	–	7.61
NM_031260	Mov10l1	Moloney leukemia virus 10-like 1	4.83	–
NM_010823	Mpl	Myeloproliferative leukemia virus oncogene	4.77	–
NM_031881	Nedd4l	Neural precursor cell expressed, developmentally down-regulated gene 4-like	3.76	–
NM_139144	Ogt	O-linked N-acetylglucosamine (GlcNAc) transferase (UDP-N-acetylglucosamine: polypeptide-N-acetylglucosaminyl transferase)	3.02	–
AY033991	Plcd4	Phospholipase C, delta 4	4.55	–
NM_008884	Pml	Promyelocytic leukemia	4.5	–
NM_009391	Ran	RAN, member RAS oncogene family	–	3.96
NM_011246	Rasgrp1	RAS guanyl releasing protein 1	3.43	–
NM_001081105	Rhoh	Ras homolog gene family, member H	5.73	–
NM_145452	Rasa1	RAS p21 protein activator 1	–	3.31
NM_172525	Arhgap29	Rho GTPase activating protein 29	–	5.05
NM_015830	Solh	Small optic lobes homolog (Drosophila)	4.86	–
NM_028004	Ttn	Titin	4.77	–
NM_011529	Tank	TRAF family member-associated Nf-kappa B activator	–	6.11
NM_009541	Zbtb17	Zinc finger and BTB domain containing 17	5.46	–
NM_008717	Zfml	Zinc finger, matrin-like	3.36	–
Kinases				
NM_134079	Adk	Adenosine kinase	–	4.07
NM_007561	Bmpr2	Bone morphogenic protein receptor, type II (serine/threonine kinase)	–	6.14
NM_001025439	Camk2d	Calcium/calmodulin-dependent protein kinase II, delta	–	4.6
NM_001042634	Clk1	CDC-like kinase 1	–	3.61
NM_007714	Clk4	CDC like kinase 4	–	3.33
NM_001109626	Crkrs	Cdc2-related kinase, arginine/serine-rich	–	7.33
NM_009974	Csnk2a2	Casein kinase 2, alpha prime polypeptide	6.07	–
XM_979562	Etnk1	Ethanolamine kinase 1	–	3.19
NM_019827	Gsk3b	Glycogen synthase kinase 3 beta	–	4.47
NM_010367	Magi1	Membrane associated guanylate kinase, WW and PDZ domain containing 1	3.12	–
NM_015823	Magi2	Membrane associated guanylate kinase, WW and PDZ domain containing 2		6.15
NM_009157	Map2k4	Mitogen activated protein kinase kinase 4	–	3.31
NM_011946	Map3k2	Mitogen activated protein kinase kinase kinase 2	–	5.02
NM_025609	Map3k7ip1	Mitogen-activated protein kinase kinase kinase 7 interacting protein 1	3.04	3.93
NM_008696	Map4k4	Mitogen-activated protein kinase kinase kinase kinase 4	3.54	–
NM_201519	Map4k5	Mitogen-activated protein kinase kinase kinase kinase 5	–	3.28
NM_011161	Mapk11	Mitogen-activated protein kinase 11	–	10.9
NM_172632	Mapk4	Mitogen-activated protein kinase 4	3.51	–
NM_015806	Mapk6	Mitogen-activated protein kinase 6	3.53	–
NM_010878	Nck1	Non-catalytic region of tyrosine kinase adaptor protein 1	–	4.24
NM_010879	Nck2	Non-catalytic region of tyrosine kinase adaptor protein 2	3.38	–
NM_021605	Nek7	NIMA (never in mitosis gene a)-related expressed kinase 7	–	3.13
NM_008702	Nlk	Nemo like kinase	–	3.99
NM_172783	Phka2	Phosphorylase kinase alpha 2	3.07	–

(Continued)

GenBank accession No	Gene symbol	Gene title	Prostate 3 h[a]	Prostate 12 h[b]
NM_011083	Pik3c2a	Phosphatidylinositol 3-kinase, C2 domain containing, alpha polypeptide	–	5.18
NM_008839	Pik3ca	Phosphatidylinositol 3-kinase, catalytic, alpha polypeptide	–	3.92
NM_008862	Pkia	Protein kinase inhibitor, alpha	–	3.28
NM_008855	Prkcb1	Protein kinase C, beta 1	–	3.34
NM_029239	Prkcn	Protein kinase C, nu	3.93	–
NM_001013833	Prkg1	Protein kinase, cGMP-dependent, type I	3.31	–
NM_007982	Ptk2	PTK2 protein tyrosine kinase 2	3.47	–
NM_009184	Ptk6	PTK6 protein tyrosine kinase 6	4.66	–
NM_009071	Rock1	Rho-associated coiled-coil containing protein kinase 1	–	4.71
NM_009072	Rock2	Rho-associated coiled-coil containing protein kinase 2	–	4.42
NM_148945	Rps6ka3	Ribosomal protein S6 kinase polypeptide 3	–	8.82
NM_028259	Rps6kb1	Ribosomal protein S6 kinase, polypeptide 1	–	3.36
NM_019635	Stk3	Serine/threonine kinase 3 (Ste20, yeast homolog)	–	3.03
NM_144825	Taok1	TAO kinase 1	–	3.93
XM_001474897	Tnik	TRAF2 and NCK interacting kinase	4.01	8.1
NM_010633	Uhmk1	U2AF homology motif (UHM) kinase 1	3.19	–
NM_030724	Uck2	Uridine-cytidine kinase 2	4.1	–
NM_198703	Wnk1	WNK lysine deficient protein kinase 1	–	6.45
Metal ion binding				
NM_009530	Atrx	Alpha thalassemia/mental retardation syndrome X-linked homolog (human)	–	4.12
NM_013476	Ar	Androgen receptor	3.23	–
NM_133738	Antxr2	Anthrax toxin receptor 2	–	3.15
AB088408	Atp6v0d1	ATPase, H^+ transporting, lysosomal V0 subunit D1	6.95	–
NM_139294	Braf	Braf transforming gene	–	3.67
NM_153788	Centb1	Centaurin, beta 1	–	6.1
NM_007805	Cyb561	Cytochrome b-561	5.53	–
NM_010006	Cyp2d9	Cytochrome P450, family 2, subfamily d, polypeptide 9	3.28	–
NM_027816	Cyp2u1	Cytochrome P450, family 2, subfamily u, polypeptide 1	5.7	–
NM_011935	Esrrg	Estrogen-related receptor gamma	3.85	–
NM_025923	Fancl	Fanconi anemia, complementation group L	–	3.38
NM_053242	Foxp2	Forkhead box P2	–	4.42
NM_026148	Lims1	LIM and senescent cell antigen-like domains 1	–	4.31
NM_008636	Mtf1	Metal response element binding transcription factor 1	15.93	–
NM_028757	Nebl	Nebulette	4.66	–
NM_152229	Nr2e1	Nuclear receptor subfamily 2, group E, member 1	11.85	–
NM_030676	Nr5a2	Nuclear receptor subfamily 5, group A, member 2	4.12	–
NM_010264	Nr6a1	Nuclear receptor subfamily 6, group A, member 1	10.31	–
NM_026000	Psmd9	Proteasome (prosome, macropain) 26S subunit, non-ATPase, 9	3.96	–
NM_177167	Ppm1e	Protein phosphatase 1E (PP2C domain containing)	3.56	–
NM_009088	Rpo1-4	RNA polymerase 1–4	4.87	4.31
NM_001103157	Steap2	Six transmembrane epithelial antigen of prostate 2	–	3.76
NM_009380	Thrb	Thyroid hormone receptor beta	–	4.67
NM_009371	Tgfbr2	Transforming growth factor, beta receptor II	4.54	–
Phosphatases				
NM_008960	Pten	Phosphatase and tensin homolog	–	3.05
NM_027892	Ppp1r12a	Protein phosphatase 1, regulatory (inhibitor) subunit 12A	–	3.77
NM_008913	Ppp3ca	Protein phosphatase 3, catalytic subunit, alpha isoform	–	9.33
NM_182939	Ppp4r2	Protein phosphatase 4, regulatory subunit 2	–	3.39
NM_011200	Ptp4a1	Protein tyrosine phosphatase 4a1	–	3.11
NM_008979	Ptpn22	Protein tyrosine phosphatase, non-receptor type 22 (lymphoid)	–	3.65
NM_001014288	Ptprd	Protein tyrosine phosphatase, receptor type, D	–	6.2
NM_025760	Ptplad2	Protein tyrosine phosphatase-like A domain containing 2	–	4.42
NM_130447	Dusp16	Dual specificity phosphatase 16	–	5.97
NM_177730	Impad1	Inositol monophosphatase domain containing 1	–	3.72

(Continued)

GenBank accession No	Gene symbol	Gene title	Prostate 3 h[a]	Prostate 12 h[b]
NM_011210	Ptprc	Protein tyrosine phosphatase, receptor type, C	4.33	–
Transcription factors and interacting partners				
AY902311	Atf2	Activating transcription factor 2	–	8.21
AY903215	Atf7ip2	Activating transcription factor 7 interacting protein 2	–	9.83
NM_001025392	Bclaf1	BCL2-associated transcription factor 1	–	3.78
NM_015826	Dmrt1	Doublesex and mab-3 related transcription factor 1	–	6.96
NM_009210	Hltf	Helicase-like transcription factor	–	3.93
NM_033322	Lztfl1	Leucine zipper transcription factor-like 1	–	4.08
NM_172153	Lcorl	Ligand dependent nuclear receptor corepressor-like	–	3.68
NM_183355	Pbx1	Pre B-cell leukemia transcription factor 1	–	5.26
NM_001018042	Sp3	Trans-acting transcription factor 3	–	3.65
AM295492	Sp6	Trans-acting transcription factor 6	–	32.91
NM_013685	Tcf4	Transcription factor 4	–	3.84
NM_178254	Tcfl5	Transcription factor-like 5 (basic helix-loop-helix)	–	4.6
NM_016767	Batf	Basic leucine zipper transcription factor, ATF-like	–	3.89
NM_001109661	Bach2	BTB and CNC homology 2	–	4.89
NM_133828	Creb1	cAMP responsive element binding protein 1	–	5.33
NM_001005868	Erbb2ip	Erbb2 interacting protein	–	3.66
NM_008031	Fmr1	Fragile X mental retardation syndrome 1 homolog	–	3.96
NM_010431	Hif1a	Hypoxia inducible factor 1, alpha subunit	–	8.62
NM_009951	Igf2bp1	Insulin-like growth factor 2 mRNA binding protein 1	5.27	–
NM_027910	Klhdc3	Kelch domain containing 3	3.33	–
NM_172154	Lcor	Ligand dependent nuclear receptor corepressor	–	3.25
NM_001005863	Mtus1	Mitochondrial tumor suppressor 1	3.29	–
NM_001081445	Ncam1	Neural cell adhesion molecule 1	3.08	–
AY050663	Nfat5	Nuclear factor of activated T-cells 5	–	4.4
NM_010903	Nfe2l3	Nuclear factor, erythroid derived 2, like 3 (Nrf3)	–	3.03
NM_001024205	Nufip2	Nuclear fragile X mental retardation protein interacting protein 2	–	4.4
NM_010881	Ncoa1	Nuclear receptor coactivator 1	3.55	3.36
NM_172495	Ncoa7	Nuclear receptor coactivator 7	–	4.46
NM_011308	Ncor1	Nuclear receptor co-repressor 1	–	5.37
NM_011544	Tcf12	Transcription factor 12	–	6.06
Transferases				
NM_144807	Chpt1	Choline phosphotransferase 1	–	4.13
NM_133869	Cept1	Choline/ethanolaminephosphotransferase 1	–	5.65
NM_030225	Dlst	Dihydrolipoamide S-succinyltransferase (E2 component of 2-oxo-glutarate complex)	–	4.04
NM_028087	Gcnt3	Glucosaminyl (N-acetyl) transferase 3, mucin type	–	7.23
NM_028108	Nat13	N-acetyltransferase 13	–	4.05
NM_008708	Nmt2	N-myristoyltransferase 2	–	4.07
NM_027869	Pnpt1	Polyribonucleotide nucleotidyltransferase 1	–	3.04
NM_172627	Pggt1b	Protein geranylgeranyltransferase type I, beta subunit	–	5.61
NM_183028	Pcmtd1	Protein-L-isoaspartate (D-aspartate) O-methyltransferase domain containing	–	7.36
NM_028604	Trmt11	tRNA methyltransferase 11 homolog (S cerevisiae)	–	3.67
NM_144731	Galnt7	UDP-N-acetyl-alpha-D-galactosamine: polypeptide N-acetylgalactosaminyltransferase 7	–	3.06
NM_172829	St6gal2	Beta galactoside alpha 2,6 sialyltransferase 2	–	3.22
NM_009178	St3gal4	ST3 beta-galactoside alpha-2,3-sialyltransferase 4	–	8.11
NM_011674	Ugt8a	UDP galactosyltransferase 8A	–	13.64
Ubiquitination				
XM_001478436	Fbxl17	F-box and leucine-rich repeat protein 17	–	3.86
NM_016736	Nub1	Negative regulator of ubiquitin-like proteins 1	3.57	–
NM_146003	Senp6	SUMO/sentrin specific peptidase 6	–	4.5
NM_016723	Uchl3	Ubiquitin carboxyl-terminal esterase L3 (ubiquitin thiolesterase)	–	6.71
NM_173010	Ube3a	Ubiquitin protein ligase E3A	–	3.12

(Continued)

GenBank accession No	Gene symbol	Gene title	Prostate 3 h[a]	Prostate 12 h[b]
NM_009481	Usp9x	Ubiquitin specific peptidase 9, X chromosome	–	3.47
NM_152825	Usp45	Ubiquitin specific petidase 45	–	3.09
NM_023585	Ube2v2	Ubiquitin-conjugating enzyme E2 variant 2	–	5.5
NM_172300	Ube2z	Ubiquitin-conjugating enzyme E2Z (putative)	3.41	–
NM_177327	Wwp1	WW domain containing E3 ubiquitin protein ligase 1	–	3.9
Others				
NM_007462	Apc	Adenomatosis polyposis coli	–	5.42
NM_021456	Ces1	Carboxylesterase 1	4.09	–
NM_021369	Chrna6	Cholinergic receptor, nicotinic, alpha polypeptide 6	4.25	–
NM_028870	Cltb	Clathrin, light polypeptide (Lcb)	22.37	–
NM_016716	Cul3	Cullin 3	–	3.2
NM_010076	Drd1a	Dopamine receptor D1A	12.13	–
NM_001033360	Gpr101	G protein-coupled receptor 101	4.26	–
NM_008211	H3f3b	H3 histone, family 3B	3.47	–
NM_008285	Hrh1	Histamine receptor H 1	10.24	–
NM_133892	Lao1	L-amino acid oxidase 1	3.39	–
NM_020280	Magea4	Melanoma antigen, family A, 4	22.06	–
NM_175632	Oscar	Osteoclast associated receptor	3.36	–
NM_009419	Tpst2	Protein-tyrosine sulfotransferase 2	7.76	–
NM_146255	Slc1a7	Solute carrier family 1 (glutamate transporter), member 7	9.36	–
NM_009206	Slc4a1ap	Solute carrier family 4 (anion exchanger), member 1, adaptor protein	–	3.27
NM_022025	Slc5a7	Solute carrier family 5 (choline transporter), member 7	9.51	–
NM_177909	Slc9a9	Solute carrier family 9 (sodium/hydrogen exchanger), isoform 9	4.23	–
NM_011506	Sucla2	Succinate-Coenzyme A ligase, ADP-forming, beta subunit	5.02	–
NM_009409	Top2b	Topoisomerase (DNA) II beta		3.3

[a] Relative mRNA expression levels of genes that were suppressed >3-fold by SFN+EGCG combination in prostate of Nrf2 wild-type mice but not in prostate of Nrf2 knockout mice compared with vehicle treatment at 3 h.

[b] Relative mRNA expression levels of genes that were suppressed >3-fold by SFN+EGCG combination in prostate of Nrf2 wild-type mice but not in prostate of Nrf2 knockout mice compared with vehicle treatment at 12 h.

in combination, we performed *in vitro* studies in PC-3 AP-1 PCa cells, *in vivo* studies in the prostate of Nrf2-deficient mice, and *in silico* bioinformatic analyses to elucidate conserved motifs in the promoter regions of these transcription factors, as well as genes coregulated by them.

We have previously reported[48] that the peak plasma concentration (C_{max}) achievable with SFN in rats was 20 μmol/L after oral administration. In addition, we have reported[49] that SFN 50 μmol/L was toxic to HepG2 C8 cells, whereas SFN 25 μmol/L was suboptimal in its efficacy. Since a desirable objective of using combinatorial approaches is to reduce the dose of the administered agents thereby reducing toxic side-effects, our dose selection of 25 μmol/L of SFN for the current study was guided by its proximity to the observed C_{max} and its suboptimal effectiveness in eliciting transcriptional effects as compared to higher doses of SFN. Besides, in most studies, the concentrations needed to observe the activities of EGCG typically range from 1 to 100 μmol/L; these are, in reality, concentrations that exceed those found in rodent and human plasma by 10- to 100-fold[50, 51]. However, the uptake of EGCG in HT-29 cells has also been shown to be concentration-dependent in the range of 20–600 μmol/L[50]. In addition, we have also previously reported[33] that EGCG inhibited HT-29 cell growth with an IC_{50} of approximately 100 μmol/L. Accordingly, we elected to test two doses of EGCG (20 and 100 μmol/L) in the current study in combination with the 25 μmol/L dose of SFN. In support of the rationale for combination regimens, a combination of atorvastatin and celecoxib has been reported to be more potent in inhibiting growth of PC-3 cells *in vitro* or grown in SCID mice than individual agents[52] for the prevention of prostate cancer. Besides, as we discussed earlier in this journal[10], our laboratory has been studying two groups of dietary phytochemical cancer-chemopreventive compounds (isothiocyanates and polyphenols), which are effective in chemical-induced, as well as genetically-induced, animal carcinogenesis models. These compounds typically generate "cellular stress" and modulate gene expression of phase II detoxifying/antioxidant enzymes. Some of the most promising members of these two classes of phytochemicals are EGCG (polyphenol) from green tea and sulforaphane (isothiocyanate) from cruciferous vegetables, hence we decided to focus on these two agents in the current study.

Interestingly, from our *in vitro* data in PC-3 AP-1 cells

(Figure 1A), we observed a diminished induction of the luciferase reporter on treatment with a combination of SFN+EGCG that was dose-dependent. We observed similar trends in our *in vivo* microarray data in Nrf2-deficient mice (Table 3), where downregulation (3-fold to around 35-fold) of key genes identified as Nrf2-dependent appeared to be the dominant response to oral administration of the SFN+EGCG combination at both 3 and 12 h. Quantitative real-time PCR analyses in our *in vitro* system (Figure 2) confirmed that several genes including ATF-2 and ELK-1 were regulated by AP-1. Bioinformatic analyses of the promoter regions of Nrf2 and AP-1, as well as ATF-2 and ELK-1, revealed an interesting group of conserved TFBS (Tables 1–2 and Figure 3) in both human and murine promoters. Furthermore, we were able to identify genes with conserved regulatory sequences in the promoter regions of human, or murine, Nrf2 and AP-1 as shown in the Supplementary Table. Indeed, microarray analyses in Nrf2-deficient mice (Table 3) confirmed that genes identified as Nrf2-dependent, including ATF-2, were coregulated with genes elicited from our AP-1 *in vitro* studies as well as the comparative analyses of promoter regions of Nrf2 and AP-1 using bioinformatic approaches. It has been noted[47] that a majority of prostate cancers contain fusion genes that result in regulation via ETS family transcription factors. Our in silico results (Tables 1–2 and Supplementary Table) as well as our *in vitro* qRT-PCR data (Figure 2) also demonstrate a role for ETS family members including ELK-1 which is, thus, in consonance with previous reports.

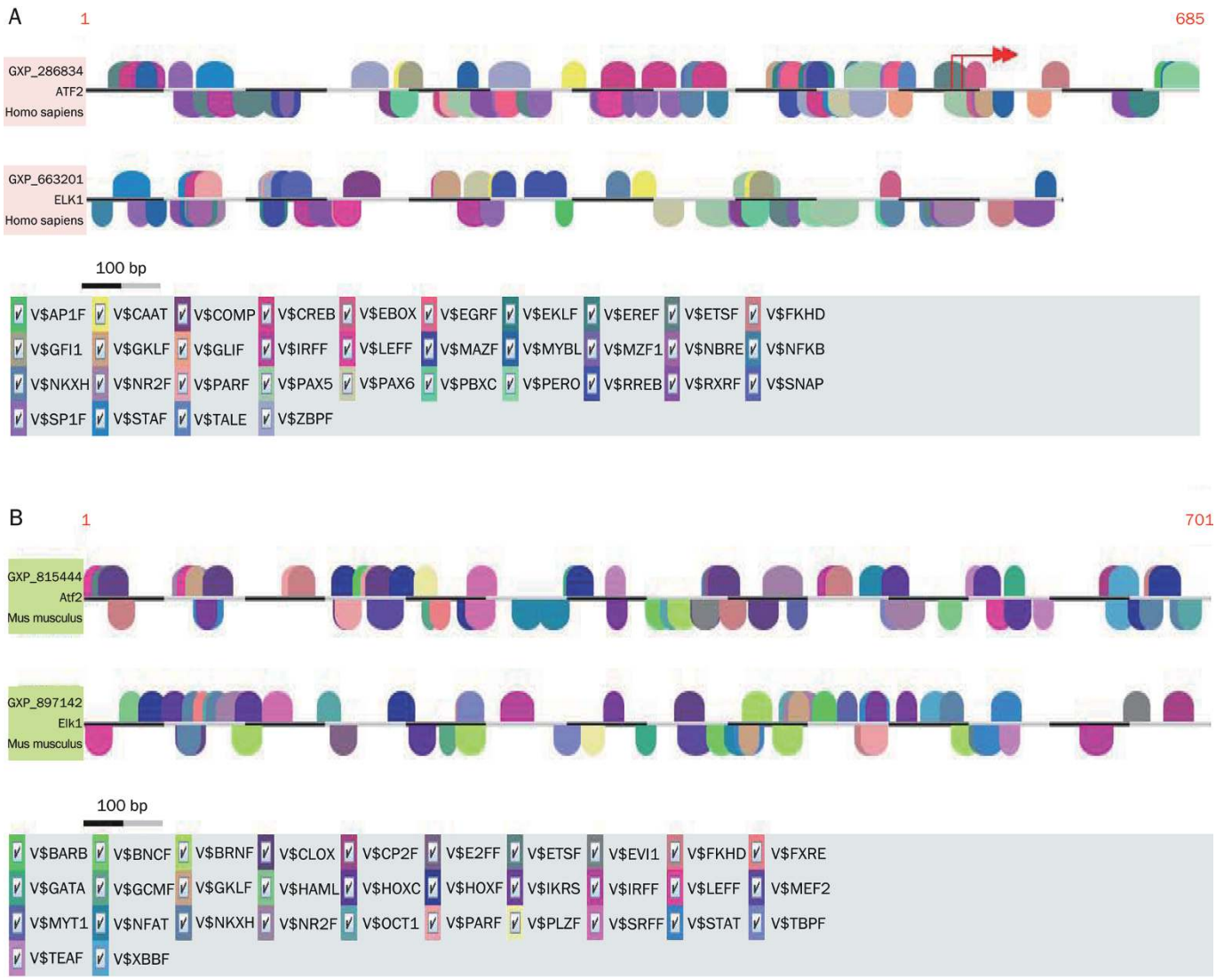

Figure 3. Conserved transcription factor binding sites (TFBS) in promoter regions of ATF-2 and ELK-1. Human promoter sequences of ATF-2 and ELK-1, or corresponding murine promoter sequences, were retrieved from Gene2Promoter (Genomatix). Comparative promoter analyses were then performed by input of these sequences in FASTA format into MatInspector using optimized default matrix similarity thresholds. The similar and/or functionally related TFBS were grouped into 'matrix families' and graphical representations of common TFBS were generated (Figure 3A, human ATF-2 and ELK-1; Figure 3B, murine Atf-2 and Elk-1). The 'V$' prefixes to the individual matrices are representative of the Vertebrate MatInspector matrix library.

The identification of conserved TFBS for pro-survival transcription factor NF-κB in the promoter regions of Nrf2 and AP-1 (Tables 1–2, Supplementary Table and Figure 3) raises an important question as to whether there could be any possible crosstalk between Nrf2, AP-1, and NF-κB in concert that may contribute to the overall effects of the SFN+EGCG combination in PCa. Indeed, further studies would be necessary to explore this possibility in greater detail. The identification of several key MAPK genes in our microarray studies (Table 3) as Nrf2-dependent is in congruence with the known role(s) of MAPKs in Nrf2 phosphorylation and activation. Besides, the downregulation of Nrf3, a negative regulator of ARE-mediated gene expression[53] with substantial homology to Nrf2, in our microarray data (Table 3) reinforces the putative chemopreventive potential of the SFN+EGCG combination. Furthermore, the elucidation of several coactivators and corepressors as Nrf2-dependent, including nuclear receptor coactivators 1 and 7 (Ncoa1 and Ncoa7) and nuclear receptor corepressor 1 (Ncor1), indicated that these cofactors may have a potentially significant role to play in the ability of Nrf2 to crosstalk with AP-1 *in vivo*.

Given the biological complexity of PCa and the need for identification of better targets, the various potential biomarkers elicited in this study may be adapted into early discovery screens for chemopreventive or chemotherapeutic intervention in PCa. The current transcriptional regulation study is a first step in understanding putative crosstalk between Nrf2 and AP-1 in PCa that may potentially be exploited by intervention with dietary phytochemicals SFN and EGCG in combination to delay the onset of clinically-evident PCa, or to arrest progression of high-grade prostate intraepithelial neoplasia (HG-PIN) to metastatic hormone-refractory prostate cancer (HRPC). Future goals include dissecting the functional biological networks for cross-talk between Nrf2 and AP-1 that will throw light on specific target hubs that play major role(s) in this cross-talk including a role(s) for potential party hubs and date hubs that might be important in this process[54–56]. Indeed, further studies focusing on the specific signaling intermediates, as well as clinical studies, would eventually be necessary to better appreciate the putative role(s) of the combination of dietary factors SFN and EGCG in the management of PCa.

Acknowledgements

This work was supported in part by RO1-CA118947 and RO1-CA094828 to Ah-Ng Tony KONG, and R21-CA133675 to Li CAI from the National Institutes of Health (NIH).

Author contribution

Sujit NAIR, Li CAI, and Ah-Ng KONG conceived and designed the study; Sujit NAIR performed the *in vitro* studies, processing of *in vivo* samples and assays on *in vivo* samples; Avantika BARVE, Tin-Oo KHOR, Guo-xiang SHEN, and Wen LIN dosed the animals with phytochemicals and sacrificed them; Sujit NAIR, Avantika BARVE, Tin-Oo KHOR, Guo-xiang SHEN, and Wen LIN harvested the prostate samples after dissection; Sujit NAIR and Li CAI performed the in silico studies and microarray analyses; Jefferson Y CHAN provided the first generation of Nrf2-knockout mice; Sujit NAIR, Li CAI, and Ah-Ng KONG analyzed the data; Sujit NAIR wrote the manuscript with contributions from Li CAI and Ah-Ng KONG; Li CAI and Ah-Ng KONG edited the manuscript; Ah-Ng KONG provided the funding support for the studies.

Abbreviations

Nrf2, Nuclear Factor-E2-related factor 2; AP-1, activator protein-1; ATF-2, activating transcription factor 2; SFN, sulforaphane; EGCG, (–)epigallocatechin-3-gallate; MAPK, mitogen-activated protein kinase; qRT-PCR, quantitative real-time PCR; TFBS, Transcription Factor Binding Sites.

Supplementary Information

Supplementary table is available at Acta Pharmacologica Sinica website of NPG.

References

1 Centers for Disease Control and Prevention (CDC). Department of Health and Human Services. Available at http://www.cdc.gov/cancer/prostate/basic_info/
2 US Cancer Statistics Working Group. United States Cancer Statistics: 2003 Incidence and Mortality. Atlanta (GA). Department of Health and Human Services, Centers for Disease Control and Prevention, and National Cancer Institute; 2007.
3 National Cancer Institute (NCI). Surveillance Epidemiology and End Results (SEER). Available at http://seer.cancer.gov/statfacts/html/prost.html
4 Scholz M, Lam R, Strum S, Jennrich R, Johnson H, Trilling T. Prostate cancer-specific survival and clinical progression-free survival in men with prostate cancer treated intermittently with testosterone inactivating pharmaceuticals. Urology 2007; 70: 506–10.
5 Welch HG, Fisher ES, Gottlieb DJ, Barry MJ. Detection of prostate cancer via biopsy in the Medicare-SEER population during the PSA era. J Natl Cancer Inst 2007; 99: 1395–400.
6 Alam J, Stewart D, Touchard C, Boinapally S, Choi AM, Cook JL. Nrf2, a Cap'n'Collar transcription factor, regulates induction of the heme oxygenase-1 gene. J Biol Chem 1999; 274: 26071–8.
7 McMahon M, Itoh K, Yamamoto M, Chanas SA, Henderson CJ, McLellan LI, *et al*. The Cap'n'Collar basic leucine zipper transcription factor Nrf2 (NF-E2 p45-related factor 2) controls both constitutive and inducible expression of intestinal detoxification and glutathione biosynthetic enzymes. Cancer Res 2001; 61: 3299–307.
8 Thimmulappa RK, Mai KH, Srisuma S, Kensler TW, Yamamoto M, Biswal S. Identification of Nrf2-regulated genes induced by the chemopreventive agent sulforaphane by oligonucleotide microarray. Cancer Res 2002; 62: 5196–203.
9 Prochaska HJ, De Long MJ, Talalay P. On the mechanisms of induction of cancer-protective enzymes: a unifying proposal. Proc Natl Acad Sci USA 1985; 82: 8232–6.
10 Nair S, Li W, Kong AN. Natural dietary anti-cancer chemopreventive compounds: redox-mediated differential signaling mechanisms in cytoprotection of normal cells versus cytotoxicity in tumor cells. Acta Pharmacol Sin 2007; 28: 459–72.
11 Yates MS, Kensler TW. Keap1 eye on the target: chemoprevention of liver cancer. Acta Pharmacol Sin 2007; 28: 1331–42.
12 Khor TO, Huang MT, Kwon KH, Chan JY, Reddy BS, Kong AN. Nrf2-

deficient mice have an increased susceptibility to dextran sulfate sodium-induced colitis. Cancer Res 2006; 66: 11580–4.
13 Burton NC, Kensler TW, Guilarte TR. *In vivo* modulation of the Parkinsonian phenotype by Nrf2. Neurotoxicology 2006; 27: 1094–100.
14 Rushmore TH, Morton MR, Pickett CB. The antioxidant responsive element. Activation by oxidative stress and identification of the DNA consensus sequence required for functional activity. J Biol Chem 1991; 266: 11632–9.
15 Wasserman WW, Fahl WE. Functional antioxidant responsive elements. Proc Natl Acad Sci USA 1997; 94: 5361–6.
16 Xu C, Yuan X, Pan Z, Shen G, Kim JH, Yu S, *et al*. Mechanism of action of isothiocyanates: the induction of ARE-regulated genes is associated with activation of ERK and JNK and the phosphorylation and nuclear translocation of Nrf2. Mol Cancer Ther 2006; 5: 1918–26.
17 Watai Y, Kobayashi A, Nagase H, Mizukami M, McEvoy J, Singer JD, *et al*. Subcellular localization and cytoplasmic complex status of endogenous Keap1. Genes Cells 2007; 12: 1163–78.
18 Hsu TC, Young MR, Cmarik J, Colburn NH. Activator protein 1 (AP-1)- and nuclear factor kappaB (NF-kappaB)-dependent transcriptional events in carcinogenesis. Free Radic Biol Med 2000; 28: 1338–48.
19 Xu C, Shen G, Yuan X, Kim JH, Gopalkrishnan A, Keum YS, *et al*. ERK and JNK signaling pathways are involved in the regulation of activator protein 1 and cell death elicited by three isothiocyanates in human prostate cancer PC-3 cells. Carcinogenesis 2006; 27: 437–45.
20 Shaulian E, Karin M. AP-1 as a regulator of cell life and death. Nat Cell Biol 2002; 4: E131–6.
21 Chinenov Y, Kerppola TK. Close encounters of many kinds: Fos-Jun interactions that mediate transcription regulatory specificity. Oncogene 2001; 20: 2438–52.
22 Steinmetz KA, Potter JD. Vegetables, fruit, and cancer. I. Epidemiology. Cancer Causes Control 1991; 2: 325–57.
23 Leoni O, Iori R, Palmieri S. Hydrolysis of glucosinolates using nylon-immobilized myrosinase to produce pure bioactive molecules. Biotechnol Bioeng 2000; 68: 660–4.
24 Getahun SM, Chung FL. Conversion of glucosinolates to isothiocyanates in humans after ingestion of cooked watercress. Cancer Epidemiol Biomarkers Prev 1999; 8: 447–51.
25 Traka M, Gasper AV, Smith JA, Hawkey CJ, Bao Y, Mithen RF. Transcriptome analysis of human colon Caco-2 cells exposed to sulforaphane. J Nutr 2005; 135: 1865–72.
26 Myzak MC, Tong P, Dashwood WM, Dashwood RH, Ho E. Sulforaphane retards the growth of human PC-3 xenografts and inhibits HDAC activity in human subjects. Exp Biol Med (Maywood) 2007; 232: 227–34.
27 Keum YS, Yu S, Chang PP, Yuan X, Kim JH, Xu C, *et al*. Mechanism of action of sulforaphane: inhibition of p38 mitogen-activated protein kinase isoforms contributing to the induction of antioxidant response element-mediated heme oxygenase-1 in human hepatoma HepG2 cells. Cancer Res 2006; 66: 8804–13.
28 Singh SV, Srivastava SK, Choi S, Lew KL, Antosiewicz J, Xiao D, *et al*. Sulforaphane-induced cell death in human prostate cancer cells is initiated by reactive oxygen species. J Biol Chem 2005; 280: 19911–24.
29 Herman-Antosiewicz A, Johnson DE, Singh SV. Sulforaphane causes autophagy to inhibit release of cytochrome *c* and apoptosis in human prostate cancer cells. Cancer Res 2006; 66: 5828–35.
30 Xu C, Shen G, Chen C, Gelinas C, Kong AN. Suppression of NF-kappaB and NF-kappaB-regulated gene expression by sulforaphane and PEITC through IkappaBalpha, IKK pathway in human prostate cancer PC-3 cells. Oncogene 2005; 24: 4486–95.
31 Petri N, Tannergren C, Holst B, Mellon FA, Bao Y, Plumb GW, *et al*. Absorption/metabolism of sulforaphane and quercetin, and regulation of phase II enzymes, in human jejunum *in vivo*. Drug Metab Dispos 2003; 31: 805–13.
32 Mukhtar H, Ahmad N. Mechanism of cancer chemopreventive activity of green tea. Proc Soc Exp Biol Med 1999; 220: 234–8.
33 Chen C, Shen G, Hebbar V, Hu R, Owuor ED, Kong AN. Epigallocatechin-3-gallate-induced stress signals in HT-29 human colon adenocarcinoma cells. Carcinogenesis 2003; 24: 1369–78.
34 Fang MZ, Wang Y, Ai N, Hou Z, Sun Y, Lu H, *et al*. Tea polyphenol (–)-epigallocatechin-3-gallate inhibits DNA methyltransferase and reactivates methylation-silenced genes in cancer cell lines. Cancer Res 2003; 63: 7563–70.
35 Fang M, Chen D, Yang CS. Dietary polyphenols may affect DNA methylation. J Nutr 2007; 137: 223S–8S.
36 Harper CE, Patel BB, Wang J, Eltoum IA, Lamartiniere CA. Epigallocatechin-3-Gallate suppresses early stage, but not late stage prostate cancer in TRAMP mice: mechanisms of action. Prostate 2007; 67: 1576–89.
37 Siddiqui IA, Adhami VM, Afaq F, Ahmad N, Mukhtar H. Modulation of phosphatidylinositol-3-kinase/protein kinase B- and mitogen-activated protein kinase-pathways by tea polyphenols in human prostate cancer cells. J Cell Biochem 2004; 91: 232–42.
38 Adhami VM, Malik A, Zaman N, Sarfaraz S, Siddiqui IA, Syed DN, *et al*. Combined inhibitory effects of green tea polyphenols and selective cyclooxygenase-2 inhibitors on the growth of human prostate cancer cells both *in vitro* and *in vivo*. Clin Cancer Res 2007; 13: 1611-9.
39 Shen G, Xu C, Hu R, Jain MR, Nair S, Lin W, *et al*. Comparison of (–)-epigallocatechin-3-gallate elicited liver and small intestine gene expression profiles between C57BL/6J mice and C57BL/6J/Nrf2(–/–) mice. Pharm Res 2005; 22: 1805–20.
40 Sang S, Yang I, Buckley B, Ho CT, Yang CS. Autoxidative quinone formation *in vitro* and metabolite formation *in vivo* from tea polyphenol (–)-epigallocatechin-3-gallate: studied by real-time mass spectrometry combined with tandem mass ion mapping. Free Radic Biol Med 2007; 43: 362–71.
41 Yu X, Kensler T. Nrf2 as a target for cancer chemoprevention. Mutat Res 2005; 591: 93–102.
42 Quandt K, Frech K, Karas H, Wingender E, Werner T. MatInd and MatInspector: new fast and versatile tools for detection of consensus matches in nucleotide sequence data. Nucleic Acids Res 1995; 23: 4878–84.
43 Cartharius K, Frech K, Grote K, Klocke B, Haltmeier M, Klingenhoff A, *et al*. MatInspector and beyond: promoter analysis based on transcription factor binding sites. Bioinformatics 2005; 21: 2933–42.
44 Chan K, Lu R, Chang JC, Kan YW. Nrf2, a member of the NFE2 family of transcription factors, is not essential for murine erythropoiesis, growth, and development. Proc Natl Acad Sci USA 1996; 93: 13943–8.
45 Li C, Wong WH. Model-based analysis of oligonucleotide arrays: expression index computation and outlier detection. Proc Natl Acad Sci USA 2001; 98: 31–6.
46 Li C, Hung Wong W. Model-based analysis of oligonucleotide arrays: model validation, design issues and standard error application. Genome Biol 2001; 2: RESEARCH0032.
47 Masters JR. Clinical applications of expression profiling and proteomics in prostate cancer. Anticancer Res 2007; 27: 1273–6.
48 Hu R, Hebbar V, Kim BR, Chen C, Winnik B, Buckley B, *et al*. *In vivo* pharmacokinetics and regulation of gene expression profiles by isothiocyanate sulforaphane in the rat. J Pharmacol Exp Ther 2004; 310: 263–71.
49 Kim BR, Hu R, Keum YS, Hebbar V, Shen G, Nair SS, *et al*. Effects of glutathione on antioxidant response element-mediated gene expression and apoptosis elicited by sulforaphane. Cancer Res 2003;

63: 7520–5.
50 Lambert JD, Lee MJ, Diamond L, Ju J, Hong J, Bose M, *et al*. Dose-dependent levels of epigallocatechin-3-gallate in human colon cancer cells and mouse plasma and tissues. Drug Metab Dispos 2006; 34: 8–11.
51 Lambert JD, Lee MJ, Lu H, Meng X, Hong JJ, Seril DN, *et al*. Epigallocatechin-3-gallate is absorbed but extensively glucuronidated following oral administration to mice. J Nutr 2003; 133: 4172–7.
52 Zheng X, Cui XX, Avila GE, Huang MT, Liu Y, Patel J, *et al*. Atorvastatin and celecoxib inhibit prostate PC-3 tumors in immunodeficient mice. Clin Cancer Res 2007; 13: 5480–7.
53 Sankaranarayanan K, Jaiswal AK. Nrf3 negatively regulates antioxidant-response element-mediated expression and antioxidant induction of NAD(P)H:quinone oxidoreductase1 gene. J Biol Chem 2004; 279: 50810–7.
54 Han JD, Bertin N, Hao T, Goldberg DS, Berriz GF, Zhang LV, *et al*. Evidence for dynamically organized modularity in the yeast protein-protein interaction network. Nature 2004; 430: 88–93.
55 Jin G, Zhang S, Zhang XS, Chen L. Hubs with network motifs organize modularity dynamically in the protein-protein interaction network of yeast. PloS one 2007; 2: e1207.
56 Agarwal S, Deane CM, Porter MA, Jones NS. Revisiting date and party hubs: novel approaches to role assignment in protein interaction networks. PLoS Comput Biol 2010; 6: e1000817.